PQ Monitoring System for Real-Time Detection and Classification of Disturbances in a Single-Phase Power System

Tomáš Radil, Pedro M. Ramos, *Member, IEEE*, Fernando M. Janeiro, *Member, IEEE*, and A. Cruz Serra, *Senior Member, IEEE*

***Abstract*—This paper presents a system for detection and classification of power quality (PQ) voltage disturbances. The proposed system applies the following methods to detect and classify PQ disturbances: Digital filtering and mathematical morphology are used to detect and classify transients and waveform distortions, whereas for short- and long-duration disturbances (such as sags, swells, and interruptions), the analysis of the root-mean-square (RMS) value of the voltage is employed. The proposed combined approach identifies the type of disturbance and its parameters such as time localization, duration, and magnitude. The proposed system is suitable for real-time monitoring of the power system and implementation on a digital signal processor (DSP).**

***Index Terms*—Digital filters, disturbance detection, morphological operation, power quality (PQ) assessment, power system monitoring, power system transients.**

I. Introduction

POWER QUALITY (PQ) monitoring has become an important part of utility services in recent years. The PQ study involves an important step: monitoring of the actual voltage and current waveforms and the detection of the PQ disturbances that occur during the monitoring. Detected disturbances are subsequently classified, and information describing their localization, duration, and type is stored and/or displayed.

According to the IEEE 1159-1995 standard [1], the PQ disturbances can be divided into the following main categories: sags, swells, interruptions, transients, and waveform distortions (e.g., harmonics and noise). These disturbances exhibit certain distinctive characteristics that can be used for their detection and classification. The detection and classification of all PQ disturbances must be sufficiently accurate both in time and amplitude to determine the cause of the disturbance. The process also has to be robust to deal with noisy data collected from the power system.

Several approaches for automatic detection and classification of PQ disturbances have been proposed in a number of papers [2]–[5]. The process is often based on time–frequency representations such as wavelet transform [3] or the short-time Fourier transform [4], which are assisted by neural networks [2], [3] or fuzzy expert systems. Methods based on pattern recognition using support vector machines are also useful techniques for disturbance classification [5]. Other approaches apply a bank of digital filters [6] or the calculation of voltage root-mean-square (RMS) value [7]. Despite the number of methods presented in the published papers, the detection and classification problem in PQ is still an open issue.

The aim of this paper is to develop a method that is suitable for automated real-time continuous monitoring of a one-phase power system. The emphasis is, therefore, on the low computational power required to perform the necessary calculations. Stress is also laid on the possibility to detect as many categories of PQ disturbances as possible. This paper only deals with the measurement, detection, and classification of the disturbances.

The proposed method is shown to be capable of detecting PQ disturbances and accurately measuring their duration and amplitude. In addition, low computational requirements make it particularly suitable for implementation in a stand-alone digital signal processor (DSP)-based instrument for real-time continuous monitoring of the power system.

II. Event Detection and Classification

In [1], the list of categories of PQ disturbances and their typical characteristics is presented. Because of the wide range of PQ disturbance parameters (frequencies, magnitudes, and durations), it is difficult to find a single method suitable for detection of all types of PQ disturbances. For example, the commonly used wavelet transform is suitable for detection of transients but fails in the case of short- and long-duration variations (such as sags and swells, particularly those with a nonrectangular shape). In addition, for the wavelet transform to detect all types of transients, higher levels of signal decomposition are required (up to the fourth [8] or sixth level [9]), which significantly increases the computational burden and, thus, makes it unsuitable for implementation in DSP-based instruments operating in real-time conditions.

Manuscript received July 5, 2007; revised April 2, 2008. This work was supported in part by the Portuguese National Research Project Reference under Grant POSC/EEA-ESE/57708/2004 and in part under Grant IT/LA/318/2005. This paper was presented in part at the 2007 IEEE Instrumentation and Measurement Technology Conference, Warsaw, Poland, May 1–3, 2007.

T. Radil is with the Instituto de Telecomunicações, 1049-001 Lisbon, Portugal (e-mail: tomas.radil@lx.it.pt).

P. M. Ramos and A. Cruz Serra are with the Instituto de Telecomunicações, 1049-001 Lisbon, Portugal, and also with the Department of Electrical and Computer Engineering, Instituto Superior Técnico, Technical University of Lisbon, 1049-001 Lisbon, Portugal (e-mail: pedro.ramos@lx.it.pt; acserra@ist.utl.pt).

F. M. Janeiro is with the Instituto de Telecomunicações, 1049-001 Lisbon, Portugal, and also with the Universidade de Évora, 7000-671 Évora, Portugal (e-mail: fmtj@uevora.pt).

Color versions of one or more of the figures in this paper are available online at http://ieeexplore.ieee.org.

Digital Object Identifier 10.1109/TIM.2008.925345

0018-9456/$25.00 © 2008 IEEE

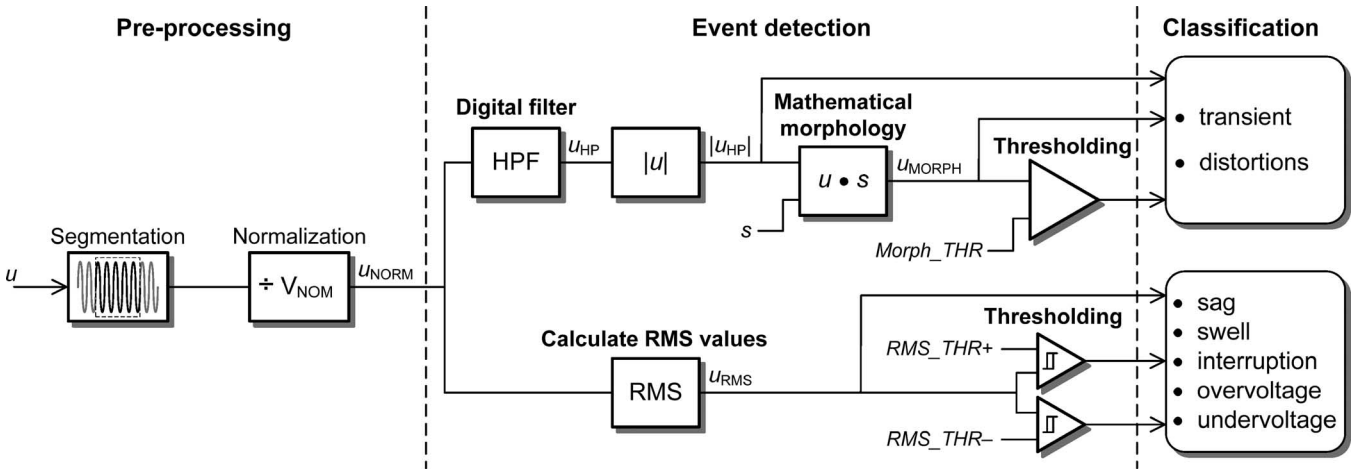


Fig. 1. Detection and classification process using the proposed method.

On the other hand, systems based only on the measurement of the voltage RMS value are not able to detect transients because during a transient, the RMS value of the voltage typically does not significantly change.

To overcome these drawbacks, a new detection-and-classification method was designed. The proposed automated method for detection and classification of PQ disturbances (also called events) does not attempt to use a single algorithm for all categories of disturbances. Instead, it uses two sets of algorithms to detect and classify various disturbances. Each set is tailored to deal with specific disturbances. For the purposes of the proposed method, the disturbances were divided into the following two groups:

1) transients and waveform distortions;
2) short- and long-duration variations (sags, swells, and interruptions).

The method consists of three major stages (see Fig. 1): pre-processing, event detection, and classification.

In the pre-processing stage, segmentation and normalization are performed. This stage is common to both groups of disturbances. In the normalization step, the input voltage waveform (in volts) is converted to a relative scale (in pu, where pu stands for per unit) by dividing the input signal by the nominal RMS voltage V_{NOM}: In our case, $V_{\mathrm{NOM}} = 230$ V. The normalization makes the following stages independent of both the power system's nominal voltage and the voltage transducer's output signal range. The output signal of the pre-processing stage u_{NORM} is then fed into the event detection stage.

After the pre-processing stage, different methods are applied to process the two groups of disturbances. The methods used in the event detection and classification stages are described in the following sections.

III. Detection and Classification of Transients and Waveform Distortions

Transients and waveform distortions (namely harmonics, interharmonics, notching, and noise) are PQ distortions with typical frequencies ranging from kilohertz up to several megahertz and magnitudes that can reach up to 8 pu [1].

The proposed method first removes, from the signal u_{NORM}, those frequency components that are not applicable for event detection (e.g., the fundamental frequency). The resulting signal u_{HP} contains features that can already be used to detect and classify PQ events. To simplify this task (e.g., by removing oscillations in the signal that would cause multiple crossings of the predefined threshold level during event detection), the features are enhanced using a mathematical morphology operation called closing.

After the closing operation, the method proceeds to event detection, which is done by thresholding the signal after closing u_{MORPH} with a predefined threshold level. The resulting signal together with the u_{MORPH} signal is used in the classification stage to distinguish between transients and waveform distortions.

The following sections describe in detail the individual steps of the proposed method.

A. Filtering

The proposed method uses a digital filter to remove those frequency components of the voltage signal that are not applicable for event detection (namely, the fundamental frequency), but depending on the application, the filter can be used to also remove other components that are of no interest to that particular application.

The solution used in this paper employs a high-pass filter (HPF in Fig. 1) that removes the lower frequencies from the voltage signal u_{NORM}. The filter is a sixth-order digital elliptic filter with a cutoff frequency of 100 Hz (which corresponds to the second harmonic of a 50-Hz power system). The gain of the filter in the passband is equal to 0 dB, and its attenuation in the stopband is 80 dB.

Fig. 2 shows the amplitude–frequency characteristic of the employed digital HPF.

B. Closing Operation

Mathematical morphology operations [10] are used for signal processing (particularly image processing) based on the signal's shape. When using mathematical morphology operations, each

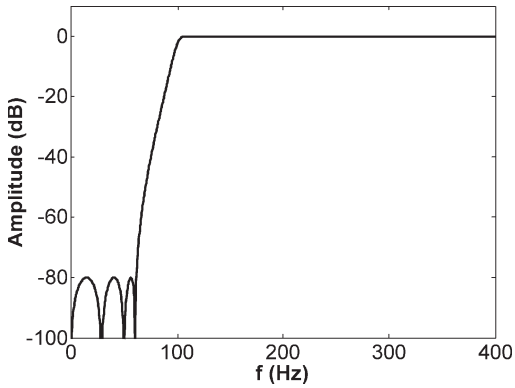


Fig. 2. Amplitude–frequency characteristic of the employed filter.

sample of the resulting signal depends on the corresponding input sample and on the samples in its neighborhood. The size and shape of the considered neighborhood are determined by a function called structuring element.

In the proposed method, the closing operation [11] is used. The closing operation is defined using two other mathematical morphology operations: 1) dilation and 2) erosion. The closing of a function u using a function s is defined as dilation $\oplus$ of u using function s followed by erosion $\ominus$ using the same function, i.e.,

$$u \bullet s = (u \oplus s) \ominus s. \tag{1}$$

Dilation is defined as

$$(u \oplus s)[n] = \max\{u[n-m]+s[m]\}, \qquad m \in S;\ n-m \in U \tag{2}$$

and erosion is defined as

$$(u \ominus s)[n] = \min\{u[n+m]-s[m]\}, \qquad m \in S,\ n+m \in U \tag{3}$$

where U and S are the domains of definition of the functions u and s, respectively. The function s is the structuring element.

In the case of the proposed method, the function to which the closing operation is applied is a 1-D signal u with length N_U, and the structuring element s is a binary vector (i.e., a vector that contains only zeros and ones) with length N_S. In such case, the definition of dilation and erosion can be written as

$$(u \oplus s)[n] = \max\{u[n-m]\}\ \forall\ s[m] \neq 0, \qquad m \in S,\ n-m \in U \tag{4}$$

$$(u \ominus s)[n] = \min\{u[n+m]\}\ \forall\ s[m] \neq 0,\ m \in S, \qquad n+m \in U \tag{5}$$

respectively, where

$$S = \begin{cases} \{-(N_S-1)/2, \ldots, (N_S-1)/2\}, & \text{if } N_S \text{ is odd} \\ \{-(N_S-2)/2, \ldots, N_S/2\}, & \text{if } N_S \text{ is even} \end{cases} \tag{6}$$

$$U = \{1, \ldots, N_U\}. \tag{7}$$

In our case, the dilation and erosion operations are thus reduced to the calculation of the maximum and minimum value of the processed signal in the neighborhood specified by the structuring element.

The closing operation is applied to the absolute value of the signal after filtering ($|u_{\mathrm{HP}}|$); the structuring element s is a vector of ones with length N_S equal to 2.5 times the period of the signal u, i.e.,

$$u_{\mathrm{MORPH}} = |u_{\mathrm{HP}}| \bullet s. \tag{8}$$

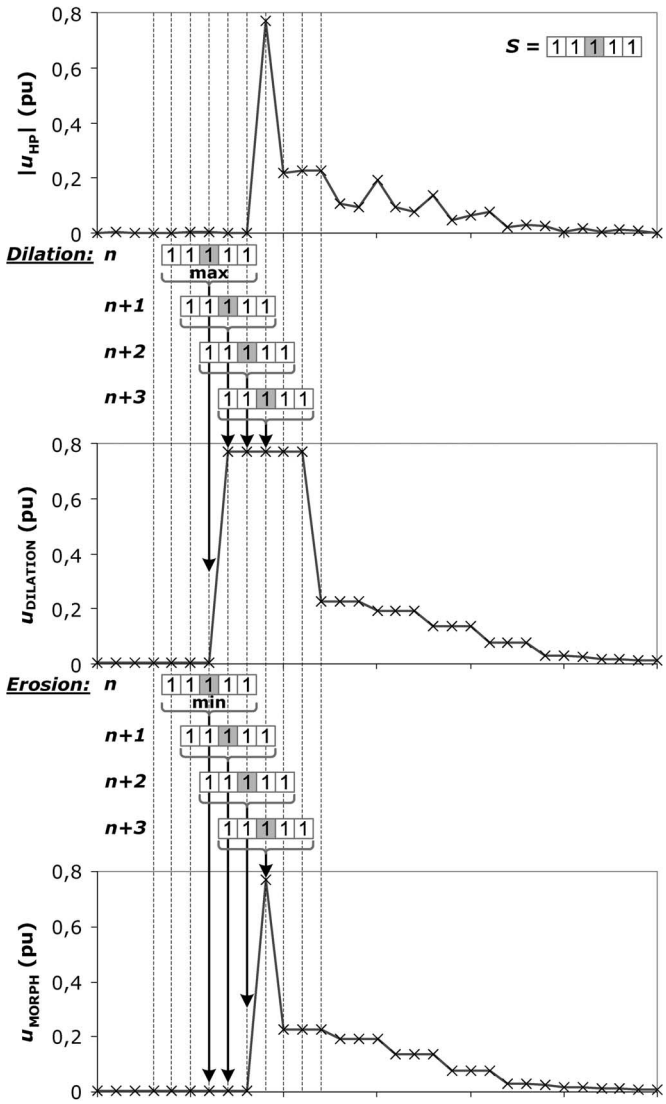


Fig. 3. Explanation of the morphology operation closing.

Application of the absolute value is necessary since the morphology operations can only work with nonnegative signals. Using the absolute value removes some information, such as the transient's polarity, from the signal. Such information, when required, has to be extracted from the u_{NORM} signal by other means.

Fig. 3 shows in detail how the output signal is calculated when using the mathematical morphology operation closing. The position of the structuring element s in four sequential calculation steps is shown in each part of the procedure. The structuring element is a vector of ones, and its length in this example is $N_S = 5$ samples. In general, the structuring element could consist of any combination of zeros and ones. For explanation purposes, a shorter structuring element and a lower sampling frequency than the ones used in the proposed method are employed in this example.

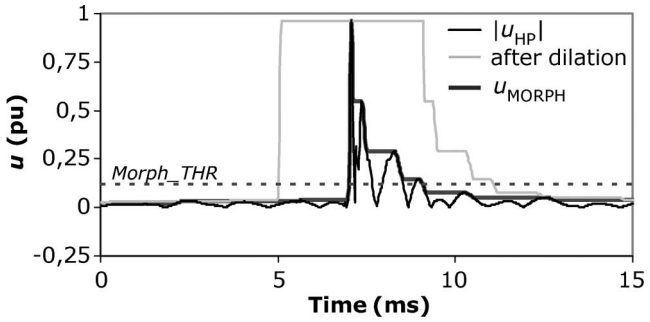


Fig. 4. Example of calculation of closing using dilation and erosion.

First, the dilation operation is calculated. Each output sample of this operation is calculated as the maximum value of the input signal $|u_{\mathrm{HP}}|$ in the neighborhood defined by the current position of the structuring element, i.e., the maximum of all the input samples that lie in the locations where the value of the structuring element is 1 is calculated. The position of the output sample is defined by the so-called origin of the structuring element, which, in Fig. 3, lies in its middle (in Fig. 3, the origin is the element with a gray background). In the next step, the structuring element is moved one sample forward, and a new output sample is calculated.

To complete the closing operation, a similar procedure is applied on the signal after dilation to calculate the erosion operation. This time, the minimum value (instead of maximum) in the neighborhood defined by the structuring element is calculated. The same structuring element as in the dilation operation is used.

Fig. 4 illustrates how the closing operation simplifies the signal after filtering and the following detection process. In addition to the signal $|u_{\mathrm{HP}}|$ and the resulting u_{MORPH} signal, the figure depicts the intermediate result after performing the dilation operation. Note that in this case, a shorter structuring element was used to simplify the explanation; in this case, N_S corresponds to 4 ms.

In Fig. 4, it can already be seen that the dilation operation removes the multiple crossings of the threshold level (Morph_THR in Fig. 4). Therefore, the signal after dilation can already be used for the detection of events. This approach of using only dilation was used earlier by the authors in [12]. Compared to performing the whole closing operation, the advantage of this solution is the smaller computational burden. Its significant drawback is the lack of accuracy of determination of the event's duration and its beginning (in both cases, the resolution is given by the length of the structuring element). These drawbacks are removed by applying the erosion operation, thus completing the closing operation. The signal after this final step (u_{MORPH}) represents the envelope of the processed signal (in this case, $|u_{\mathrm{HP}}|$), which enables simple detection of events and accurate determination of their parameters.

C. Event Detection and Classification

After the closing operation, the event detection is done by thresholding the morphology result, i.e., an event is detected when the u_{MORPH} signal exceeds the thresholding level Morph_THR. Since u_{MORPH} is proportional to the amplitude of the disturbances, the Morph_THR threshold value can be seen as the minimum disturbance amplitude to be detected. By adjusting the Morph_THR level, the algorithm's sensitivity can easily be adjusted to the required level.

TABLE I
TYPICAL PARAMETERS OF TRANSIENTS AND WAVEFORM DISTORTIONS

Disturbance	Duration	Frequency	Typ. voltage magnitude
Transient	ns – ms	5 kHz – 5 MHz	0 – 8 pu
Harmonics	steady state	0 – 5 kHz	0 – 0.2 pu
Interharmonics	steady state	0 – 6 kHz	0 – 0.02 pu
Notching	steady state		
Noise	steady state	broadband	0 – 0.01 pu

After thresholding, the proposed method proceeds to the classification stage to distinguish between transients and several types of waveform distortions (such as harmonics, interharmonics, notching, and noise) and to determine the duration and magnitude of the detected event. The classification is based on the typical parameters of the disturbances (see Table I) [1].

The proposed method assumes that if the duration of the event in the u_{MORPH} signal is longer than 2.5 times the power system voltage period (50 ms in the case of 50-Hz systems), the detected disturbance has a steady-state nature, and therefore, the disturbance is classified as waveform distortion. The duration of the event is determined as the time during which u_{MORPH} continuously exceeds the Morph_THR threshold level. The 50-ms limit is defined by the length of the structuring element used in the closing operation. The value was selected based on the typical parameters of disturbances [1]. If the character of the disturbance is steady state, there will be a single pulse in the output signal after the closing operation using this structuring element. The width of this pulse will be equal to the waveform distortion length, as will be shown in the measurement results.

If the disturbance is shorter than the 50-ms threshold, the detected event is a transient. However, in this case, the $|u_{\mathrm{HP}}|$ signal has to be processed again using the closing operation, this time with a shorter structuring element (one fifth of the voltage signal period, which is 4 ms in the case of a 50-Hz power system). The shorter structuring element enables the detection of potential transients that are close together and that (due to the long structuring element used to obtain u_{MORPH}) might have appeared as a single event.

The duration of the events is determined from the crossings of the interpolated signal after closing with the Morph_THR threshold level; the magnitude of the events is determined as the maximum value of the signal after closing during the event. Linear interpolation between samples is used to increase the precision of the determination of the event's duration and location.

D. Implementation

The method for detection of transients and waveform distortions is based on digital filtering and morphology operation closing.

An infinite impulse response (IIR) digital filter was selected to keep the filter's order low, thus reducing the computational requirements and enabling real-time operation of the proposed method. The drawback of IIR filters compared to finite impulse response (FIR) filters is their nonlinear phase. The major advantage is the IIR filter's low order required to implement a filter with a specified frequency characteristic. The IIR filter employed in this paper was of sixth order, whereas the order of an FIR filter with a similar frequency characteristic would be on the order of thousands. A similar low-order IIR filter can be designed for applications where only the fundamental needs to be removed. For example, a bandstop filter that suppresses frequencies between 47.5 and 52.5 Hz with −80-dB attenuation in the stopband can be realized as an IIR filter of the tenth order.

The calculation of the morphology operations in the example shown in Fig. 3 literally follows (1), (4), and (5). Such an approach is very inefficient. Actual implementations of the morphology operations use algorithms such as the van Herk–Gil–Werman algorithm for efficient calculation of the dilation and erosion [13], [14]. This algorithm requires $3 - 4/N_S$ comparison operations per sample of the structuring element to calculate one output sample. Therefore, for large N_S, the computational requirements of the closing operation linearly depend on the structuring element's length.

Both digital filters and morphology operations can efficiently be implemented, e.g., in MATLAB or in a DSP. The proposed method is faster than commonly used methods, such as those based on the wavelet transform [8], [9]. The processing using the proposed method (filtering, calculation of the absolute value, and calculation of the closing operation) is, on average, 20% faster than the detection using the discrete wavelet transform (Daubechies mother wavelet with four coefficients and six levels of decomposition). This result was achieved in a MATLAB implementation when processing 1200 previously stored records with transients and waveform distortions. Note that the processing speed difference is even bigger when using mother wavelets with more coefficients or higher levels of decomposition.

The proposed method was implemented in a DSP-based PQ analyzer. The analyzer is described in [15], where more detailed information on the algorithm's performance can be found.

IV. Detection and Classification of Short- and Long-Duration Variations

According to [1], short- and long-duration variations include sags, swells, interruptions, undervoltages, and overvoltages. The typical duration of these events ranges from 0.5 cycles up to more than 1 min, whereas the typical magnitudes range from 0.1 pu up to 1.8 pu.

A. Detection

The most distinctive feature of these disturbances is the change of the voltage signal's RMS value during the disturbance. The proposed method follows the recommendations of the standard [16]. In the event-detection stage, the method determines the RMS value over one period of the normalized input signal u_{NORM} and updates this value every half-period, i.e.,

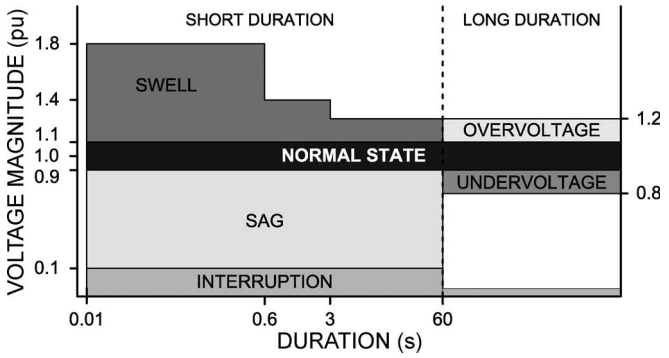


Fig. 5. Typical parameters of short- and long-duration variations.

$$u_{\mathrm{RMS}}(j) = \sqrt{\frac{1}{N}\sum_{i=(j-1)N/2}^{(j+1)N/2-1} u_{\mathrm{NORM}}^2(i)} \tag{9}$$

where N is the number of samples per period, and $j = 1, 2, \ldots, 2p-1$, where p is the number of periods in the segment that is being analyzed.

Thresholding is then applied on the resulting signal u_{RMS} to detect the events. The signal u_{RMS} is compared with two threshold levels, as shown in Fig. 1: RMS_THR− (below the nominal RMS value) and RMS_THR+ (above the nominal RMS value). The method uses hysteresis in the detection of the event's start and end to avoid the detection of false events in the case when, for example, the RMS value remains close to one of the RMS_THR levels over a period of time.

B. Classification

To distinguish between individual types of short- and long-duration variations, the minimum and maximum values of the u_{RMS} during the detected event and the duration of the event are used. Fig. 5 shows the typical parameters of individual short- and long-duration variations [1]. The values shown in Fig. 5 are typical values, and the method marks any event whose magnitude drops below 0.1 pu as an interruption; events with magnitudes between 0.1 and 0.9 pu are classified as sags or undervoltages, depending on their duration, whereas events with magnitudes above 1.1 pu are marked as swells or overvoltages, again depending on their duration.

The duration of the event is calculated as the time between the crossing of the respective RMS_THR level and the moment the signal u_{RMS} returns into the interval defined by these threshold levels. The event's magnitude is the maximum (in the case of swells and overvoltages) or the minimum (in the case of interruptions, sags, and undervoltages) value of the RMS during the event.

V. Experimental Results

A system for monitoring a single-phase power system (230 V/50 Hz) has been developed and implemented. The

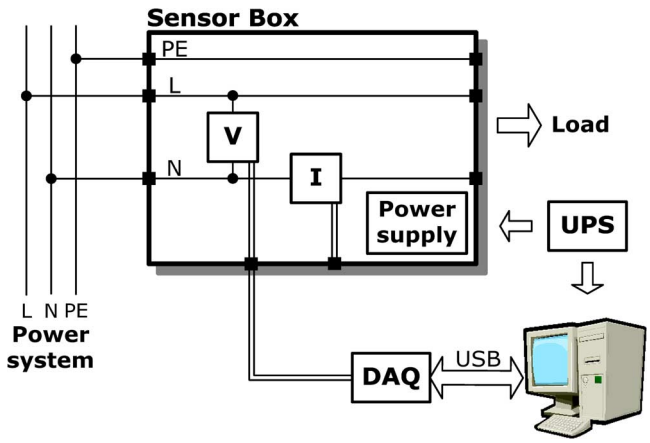


Fig. 6. PQ monitoring system.

system (Fig. 6) consists of a sensor box, a data acquisition (DAQ) board, and a PC that performs all the required processing.

The sensor box [17] contains a current transducer (LA 25-NP [18]) and a voltage transducer (LV 25-P [19]). In this paper, only the voltage transducer was used for the measurement of disturbances in the power system. Both transducers are based on closed-loop, Hall-effect sensors. The input range of the voltage transducer is 500 V. Its frequency range is from dc up to approximately 10 kHz. The maximum relative error is 0.8%. The input impedance of the voltage transducer is 27 kΩ. The current transducer has a frequency range from dc up to 150 kHz and is configured for an input range of 6 A. Its maximum relative error is 0.5%.

Due to the selected voltage transducer's bandwidth, the measuring system was not able to detect high-frequency disturbances (such as high-frequency transients). The transducer's bandwidth is sufficient to detect events such as oscillatory transients, waveform distortions caused by the presence of harmonics (up to the usual limit of fiftieth harmonic), sags, swells, and interruptions. However, the mentioned limitation is solely caused by the employed transducer and does not represent an inherent shortcoming of the proposed detection and classification method.

The sensor box was connected to the power system, and the output signal of the voltage transducer was sampled using a 16-bit DAQ board (National Instruments USB-9215) and recorded on a PC, where all the signal processing was done. Both the sensor box and the PC were powered using an uninterruptible power supply to secure proper power, even during long sags or interruptions.

Due to the bandwidth of the used voltage transducer and the memory requirements, the sampling frequency was set to 50 kS/s. In all measurements, the threshold levels were adjusted according to the values indicated in Table II.

The proposed method was tested using three types of signals:

1) simulated signals with artificial disturbances [20];
2) measured signals generated using sag and swell generator [20];

TABLE II
THRESHOLD LEVEL SETTINGS

Threshold level	Setting
Morph_THR	0.12 pu
RMS_THR–	0.9 pu
RMS_THR+	1.1 pu

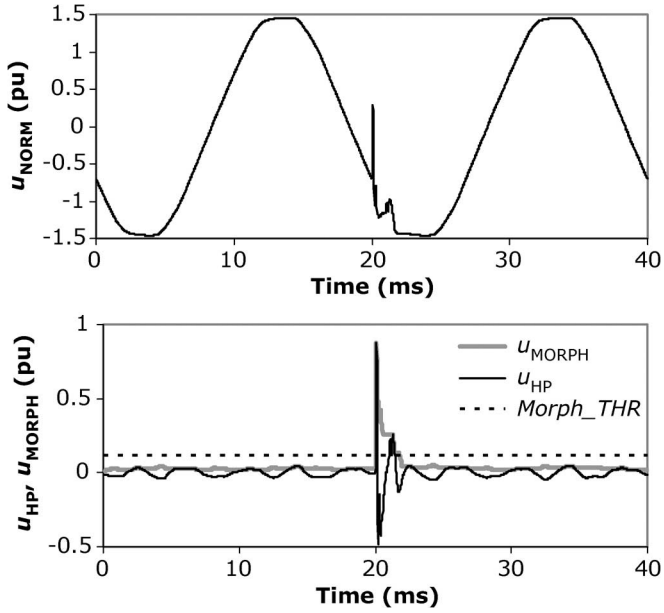


Fig. 7. Measured PQ event. Transient 1.

3) signals measured during long-term monitoring of the power grid network at different locations.

The first two types of signals were used in the initial stages of development of the proposed method, whereas long-term monitoring was used to verify performance and applicability of the method in a real environment. The following figures show some examples of signals measured in the course of monitoring.

Examples of measured transients are shown in Figs. 7–10. These figures depict the normalized voltage signal u_{NORM} and the corresponding signals u_{HP} and u_{MORPH} that were used in detection and classification. Table III shows the summary of parameters of individual transients.

The character of the first two transients (Figs. 7 and 8) is oscillatory (these transients are possibly a result of capacitor switching [21], [22]); the transients in Figs. 9 and 10 have an impulsive character.

In the following example, a waveform distortion is shown in Fig. 11, whereas the corresponding signals used in event detection are shown in Figs. 12 and 13. The distortion's duration is 0.42 s, and its peak magnitude is 0.18 pu. Only the initial part of the disturbance is shown in Figs. 11 and 12. The whole length of the signals used in detection and classification is shown in Fig. 13.

The following two sets of figures show examples of PQ disturbances from the second group of events, i.e., short- and long-duration disturbances. The first two figures (Figs. 14 and 15) depict a measured sag, namely, the measured voltage waveform, and the u_{RMS} signal used for detection and classification of

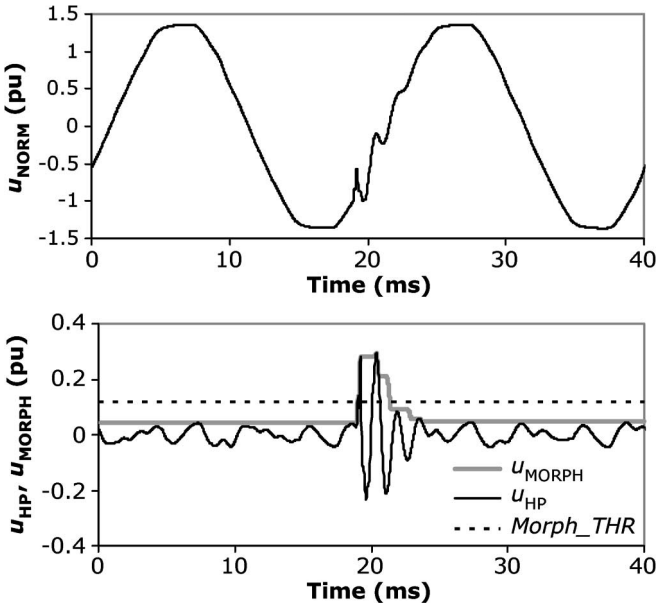


Fig. 8. Measured PQ event. Transient 2.

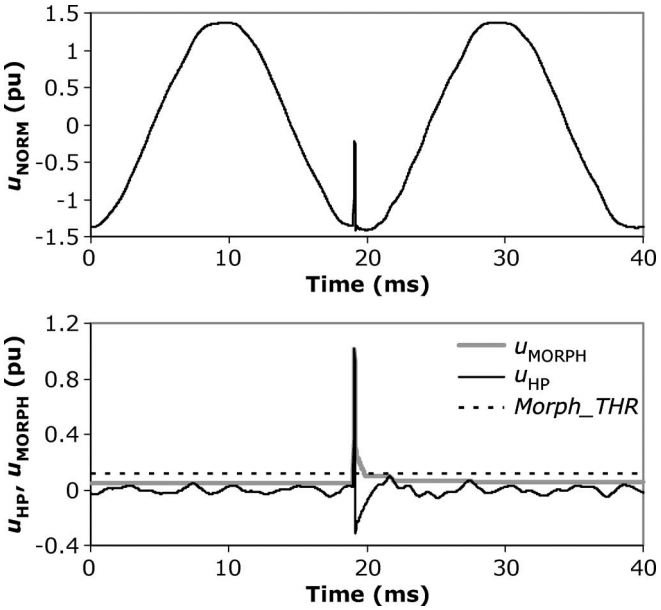


Fig. 9. Measured PQ event. Transient 3.

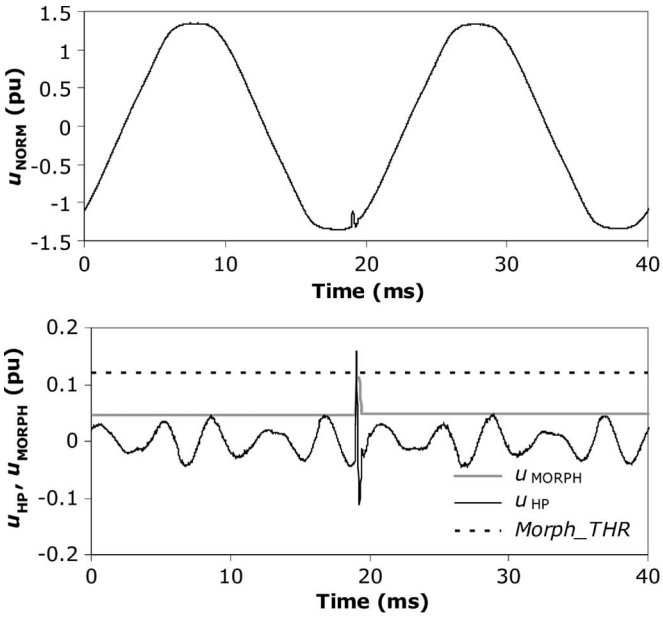


Fig. 10. Measured PQ event. Transient 4.

TABLE III
PARAMETERS OF THE MEASURED TRANSIENTS

Transient	Magnitude	Duration
#1 (Fig. 7)	0.88 pu	1.8 ms
#2 (Fig. 8)	0.30 pu	2.4 ms
#3 (Fig. 9)	1.02 pu	0.8 ms
#4 (Fig. 10)	0.16 pu	0.06 ms

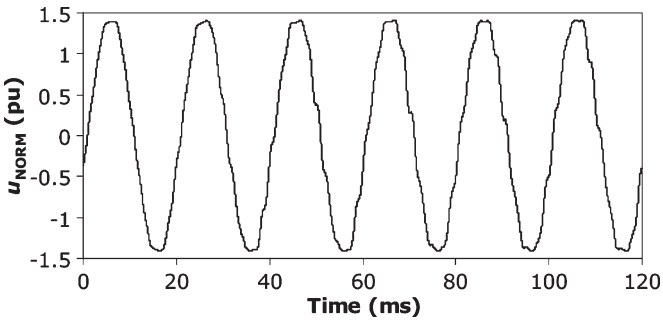


Fig. 11. Measured PQ event. Waveform distortion (detail of the voltage signal).

the disturbance. Note that due to hysteresis, the threshold level used to detect the beginning of the event is lower (at 0.9 pu, represented by a dashed line) than the threshold used to detect the event's end (at 0.92 pu, represented by a dot-dashed line), as shown in Fig. 15. The sag lasted approximately 1.35 s, and the minimum voltage magnitude during the event was 0.6 pu.

Fig. 16 shows an example of a measured interruption. From the RMS value evolution (Fig. 17), it can first be seen that the voltage slowly dropped to 0 pu. Afterward, the voltage suddenly increased, but the normal state (the RMS value above the RMS_THR level) was restored approximately 3.3 s later. The event lasted for 3.93 s and was classified as an interruption [1].

VI. CONCLUSION

An automated PQ monitoring system for real-time detection and classification of single-phase power system disturbances has been described in this paper. The system was based on a new detection-and-classification algorithm based on the categories of PQ events described by the IEEE standard [1].

The algorithm used different methods to detect and classify two groups of PQ events. For the detection of transients and waveform distortions, a digital HPF and the mathematical morphological operation closing were used. In the case of short- and long-duration variations (such as sags, swells, and interruptions), the RMS value of the voltage signal was analyzed to detect these events.

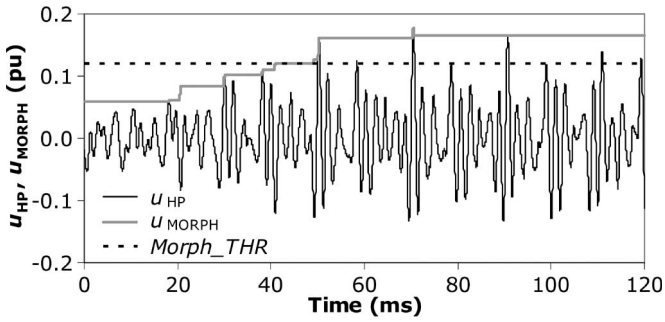


Fig. 12. Waveform distortion. Detail of the signals used in detection and classification.

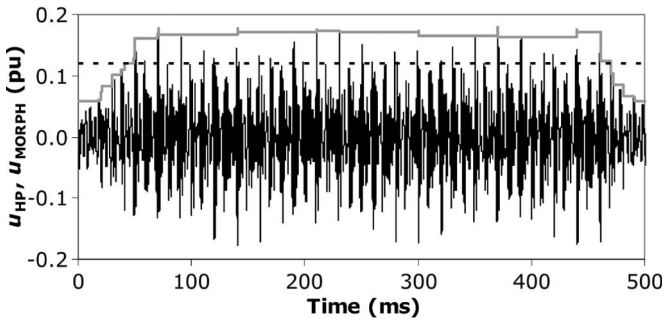


Fig. 13. Waveform distortion. Signals used in detection and classification.

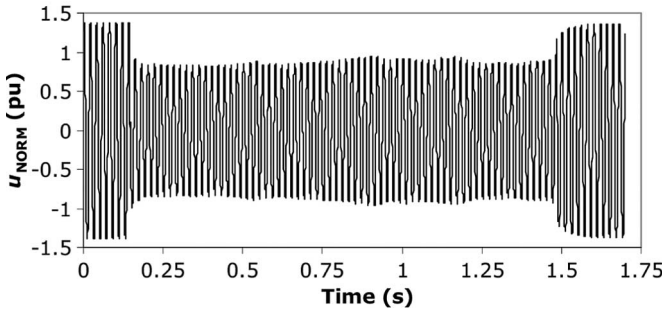


Fig. 14. Measured PQ event. Sag.

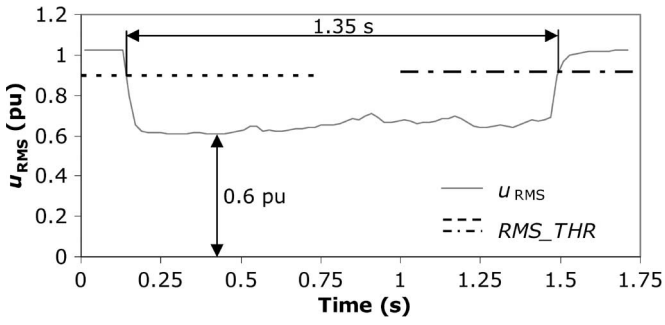


Fig. 15. Sag. Signal used in detection and classification.

The proposed method was tested using both simulated data with artificial disturbances and data measured in single-phase power systems.

All algorithms used for detection and classification are fast, simple, and suitable for implementation on a DSP. In particular, the detection stage can also be easily implemented on a field-programmable gate array or even using analog circuitry (contrary to methods based on, e.g., the wavelet transform).

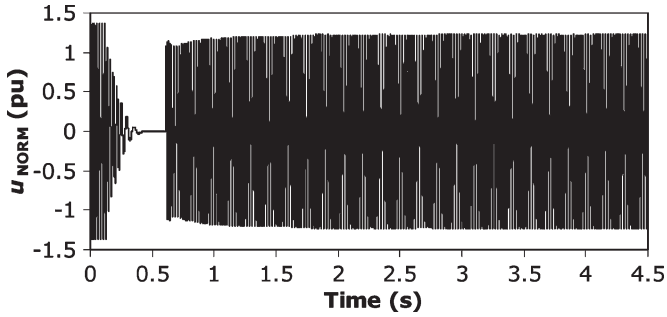


Fig. 16. Measured PQ event. Interruption.

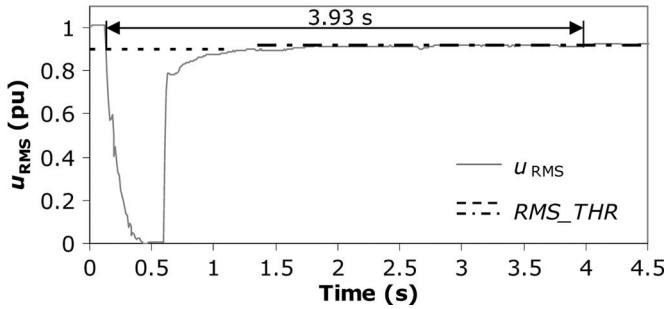


Fig. 17. Interruption. Signal used in detection and classification.

A comparison with disturbance detection using the discrete wavelet transform showed that the proposed method is faster.

Another advantage of the proposed method is the simplicity of adjustment of its sensitivity: By adjusting the threshold levels Morph_THR and RMS_THR, its sensitivity can be adjusted to the required level.

The drawbacks of the method lie in its inability to distinguish between certain categories of disturbances. For example, the method cannot distinguish between harmonics and interharmonics, and it marks all such disturbances as waveform distortions. In addition, the development has focused on the most common disturbances (transients and sags), and flicker, for example, was not yet taken into account. These issues will be addressed in the future revisions of the detection-and-classification method.

REFERENCES

[1] *IEEE Recommended Practice for Monitoring Electric Power Quality*, Nov. 1995. IEEE Std. 1159-1995.

[2] A. M. Gaouda, S. H. Kanoun, M. M. A. Salama, and A. Y. Chikhani, "Pattern recognition applications for power system disturbance classification," *IEEE Trans. Power Del.*, vol. 17, no. 3, pp. 677–683, Jul. 2002.

[3] Z.-L. Gaing, "Wavelet-based neural network for power quality disturbance recognition and classification," *IEEE Trans. Power Del.*, vol. 19, no. 4, pp. 1560–1568, Oct. 2004.

[4] M. Wang, G. I. Rowe, and A. V. Manishev, "Classification of power quality events using optimal time-frequency representations, theory and application," *IEEE Trans. Power Del.*, vol. 19, no. 3, pp. 1496–1503, Jul. 2004.

[5] F.-F. Zhu, G.-S. Hu, and J. Xie, "Classification of power quality disturbances using wavelet and fuzzy support vector machines," in *Proc. 4th Int. Conf. Mach. Learn. Cybern.*, Aug. 2005, vol. 7, pp. 3981–3984.

[6] Z. Chen and P. Urwin, "Power quality detection and classification using digital filters," in *Proc. Porto PowerTech*, Sep. 2001, vol. 1, no. 6, p. 6.

[7] E. Styvaktakis, M. H. J. Bollen, and I. Y. H. Gu, "Automatic classification of power system events using rms voltage measurements," in *Proc. Power Eng. Soc. Summer Meeting*, 2002, vol. 2, pp. 824–829.

[8] S. Santoso, E. J. Powers, W. M. Grady, and P. Hofmann, "Power quality assessment via wavelet transform analysis," *IEEE Trans. Power Del.*, vol. 11, no. 2, pp. 924–930, Apr. 1996.
[9] H. He and J. A. Starzyk, "A self-organizing learning array system for power quality classification based on wavelet transform," *IEEE Trans. Power Del.*, vol. 21, no. 1, pp. 286–295, Jan. 2006.
[10] J. Serra, *Image Analysis and Mathematical Morphology*, vol. 1. New York: Academic, 1982.
[11] J.-G. Postaire, R. D. Zhang, and C. Lecocq-Botte, "Cluster analysis by binary morphology," *IEEE Trans. Pattern Anal. Mach. Intell.*, vol. 15, no. 2, pp. 170–180, Feb. 1993.
[12] V. Matz, T. Radil, P. M. Ramos, and A. C. Serra, "Automated power quality monitoring system for on-line detection and classification of disturbances," in *Proc. IEEE Instrum. Meas. Technol. Conf.*, Warsaw, Poland, May 2007, pp. 1–6.
[13] M. van Herk, "A fast algorithm for local minimum and maximum filters on rectangular and octagonal kernels," *Pattern Recognit. Lett.*, vol. 13, no. 7, pp. 517–521, Jul. 1992.
[14] J. Y. Gil and M. Werman, "Computing 2-D min, median and max filters," *IEEE Trans. Pattern Anal. Mach. Intell.*, vol. 15, no. 5, pp. 504–507, May 1993.
[15] P. M. Ramos, T. Radil, F. M. Janeiro, and A. C. Serra, "DSP based power quality analyzer using new signal processing algorithms for detection and classification of disturbances in a single-phase power system," in *Proc. IMEKO TC4 Symp.*, Iasi, Romania, Sep. 2007, vol. II, pp. 433–438.
[16] *Electromagnetic Compatibility (EMC): Testing and Measurement Techniques—Power Quality Measurement Methods*, 2003. IEC 61000-4-30.
[17] P. M. Ramos, N. B. Brás, and A. C. Serra, "A new calibration method for current and voltage sensors used in power quality measurements," in *Proc. IMTC*, Apr. 2006, pp. 2283–2288.
[18] *Current Transducer LEM LA 25-NP*. [Online]. Available: http://web4.lem.com/docs/products/LA 25-NP E.pdf
[19] *Voltage Transducer LEM LV 25-P*. [Online]. Available: http://web4.lem.com/docs/products/LV 25-P E.pdf
[20] T. Radil, V. Matz, P. Ramos, and A. C. Serra, "Development of a real-time power quality monitoring instrument for detection and classification of disturbances in a single-phase power system," in *Proc. Conftele*, 2007, pp. 267–270.
[21] M. Forti and L. Millanta, "Power-line impedance and the origin of the low-frequency oscillatory transients," *IEEE Trans. Electromagn. Compat.*, vol. 32, no. 2, pp. 87–97, May 1990.
[22] M. H. J. Bollen and I. Y. H. Gu, *Signal Processing of Power Quality Disturbances*. Hoboken, NJ: Wiley, 2006.



Tomáš Radil was born in Hradec Králové, Czech Republic, in 1977. He received the M.S. and Ph.D. degrees in electrical engineering from Czech Technical University, Prague, Czech Republic, in 2002 and 2005, respectively.

Since 2006, he has been with the Instituto de Telecomunicações, Lisbon, Portugal, where he is currently a member of the instrumentation and measurement research line. His current research interests include power quality measurements and impedance measurement.



Pedro M. Ramos (M'02) was born in Lisbon, Portugal, on November 23, 1972. He received the Diploma, Master's, and Ph.D. degrees from the Instituto Superior Técnico (IST), Technical University of Lisbon (UTL), in 1995, 1997, and 2001, respectively, all in electrical and computer engineering.

Since 1995, he has been with the Instituto de Telecomunicações, Lisbon, where he is currently a member of the instrumentation and measurement research line. Since 1999, he has been a member of the teaching and research staff at the IST/UTL. His current research interests include impedance measurements, sine-fitting algorithms, automatic measurement systems, and power quality monitoring/ measurements.



Fernando M. Janeiro (M'04) was born in Almada, Portugal, on June 16, 1974. He received the Diploma and Ph.D. degrees in electrical and computer engineering from the Instituto Superior Técnico (IST), Technical University of Lisbon (UTL), Lisbon, Portugal, in 1997 and 2004, respectively.

Since 1997, he has been with the Instituto de Telecomunicações, Lisbon, where he is currently a member of the instrumentation and measurement research line. He is an Assistant Professor with the Department of Physics, Universidade de Évora, Évora, Portugal, where he has been a member of the teaching and research staff since 2001. His current research interests include impedance measurements, sine-fitting algorithms, power quality measurements, and environmental measurement systems.



A. Cruz Serra (M'00–SM'03) was born in Coimbra, Portugal, on December 17, 1956. He received the Diploma in electrotechnical engineering from the University of Oporto, Oporto, Portugal, in 1978 and the Master's and Ph.D. degrees in electrical and computer engineering from the Instituto Superior Técnico (IST), Technical University of Lisbon (UTL), Lisbon, Portugal, in 1985 and 1992, respectively.

He is currently a Full Professor of instrumentation and measurement with the IST/UTL, where he has been a member of the teaching and research staff since 1978. Since 1994, he has been with the Instituto de Telecomunicações, Lisbon, where he is currently a member of the instrumentation and measurement research line. His current research interests include electrical measurements, ADC modeling, testing and standardization, and automatic measurement systems.